EUROPHYSICS LETTERS 15 February 2005

Europhys. Lett., **69** (4), pp. 629–635 (2005)
DOI: 10.1209/epl/i2004-10397-8

One-bead microrheology with rotating particles

M. Schmiedeberg and H. Stark(*)
Universität Konstanz, Fachbereich Physik - D-78457 Konstanz, Germany

received 9 September 2004; accepted in final form 16 December 2004
published online 19 January 2005

PACS. 83.10.-y – Rheology: Fundamentals and theoretical.
PACS. 47.32.-y – Rotational flow and vorticity.
PACS. 83.60.Bc – Linear viscoelasticity.

Abstract. – We lay the theoretical basis for one-bead microrheology with rotating particles, *i.e.*, a method where colloids are used to probe the mechanical properties of viscoelastic media. Based on a two-fluid model, we calculate the compliance and discuss it for two cases. We first assume that the elastic and the fluid component exhibit both stick boundary conditions at the particle surface. Then, the compliance fulfills a generalized Stokes law with a complex shear modulus whose validity is only limited by inertial effects, in contrast to translational motion. Secondly, we find that the validity of the Stokes regime is reduced when the elastic network is not coupled to the particle.

Introduction. – In recent years, the experimental method of microrheology [1] emerged as a powerful tool to monitor the mechanical properties of viscoelastic soft materials [2, 3] especially in biological systems [4, 5] including cells [6]. The main idea is to disperse micron-sized beads into the material and monitor their motion either as response to external forces (active method) [6, 7] or due to Brownian fluctuations (passive method) [5, 8]. Whereas in the first method the frequency-dependent response function or compliance is measured directly, it is inferred in the second method from the particle's positional fluctuations using the fluctuation-dissipation theorem and the Kramers-Kronig relations [5].

In this article, we address the particles' rotational degree of freedom and lay the theoretical basis to use it in microrheology. To monitor the particles' orientations, they have to be anisotropic. And indeed, first experimental implementations of one-bead microrheology with either birefringent spherial particles [9] or microdisks [10] do exist.

The main theoretical problem of microrheology is how the particle compliance measured in experiments relates to the viscoelastic properties of the material quantified in its complex shear modulus. We will show here, based on a model-viscoelastic medium, the so-called two-fluid system [11], that the compliance in the rotational case obeys a generalized Stokes law which is only limited by an upper crossover frequency, in contrast to the translational motion where the validity is restricted to a frequency window [5, 12]. So one advantage of rotating particles is that they extend the frequency range that allows a straightforward interpretation of the experimental results by the Stokes law.

(*) E-mail: Holger.Stark@uni-konstanz.de

Let us first review the reason for the frequency window in the translational case [5]. As a model-viscoelastic medium, we consider an elastic component, *e.g.*, a polymer network, which can move relative to a Newtonian fluid. A particle embedded in this medium experiences an external oscillating force with amplitude $F(\omega)$ and reacts with an oscillating displacement described by the amplitude $x(\omega) = \alpha(\omega)F(\omega)$, where $\alpha(\omega)$ is the compliance as a function of frequency ω. For $\omega = 0$, the displaced particle creates a deformation field in the elastic network which includes both shear and compressional contributions. For small ω, the elastic network thus has to move relative to the incompressible fluid since the latter only allows shear motions. However, the frictional force between both components increases with their relative speed. Hence, beyond a crossover frequency ω_{c1}, elastic network and viscous fluid are strongly coupled and can be considered as a single incompressible viscoelastic medium. The compliance for a spherical particle then assumes the simple generalized Stokes relation $\alpha(\omega) = [6\pi G(\omega)a]^{-1}$, where $G(\omega) = \mu - i\omega\eta$ is the complex shear modulus, η is viscosity and μ denotes Lamé's elastic constant associated with shear. Beyond a second crossover frequency ω_{c2}, inertial effects of the fluid become important and the generalized Stokes relation is no longer valid. This scenario is confirmed by detailed calculations using a "volume localization" approximation [12]. On the other hand, a rotating particle creates a pure shear field in the elastic network for all frequencies. Hence, we expect the validity of the Stokes relation to extend to $\omega = 0$.

Theory. – In the following, we consider a rotating particle with an oscillating angular displacement $\boldsymbol{\Phi}(t) = \boldsymbol{\Phi}(\omega)e^{-i\omega t}$, where the direction of the vector $\boldsymbol{\Phi}(\omega)$ characterizes the axis of rotation. Since the pressure around the particle stays constant, the oscillating velocity field in a pure incompressible Newtonian fluid is described by the Helmholtz equation $(\nabla^2 + k^2)\boldsymbol{v}(\boldsymbol{r},\omega) = 0$ with wave number $k = \sqrt{i\omega\rho/\eta}$ [13]. Under stick boundary conditions it assumes the form

$$\boldsymbol{v}(\boldsymbol{r},\omega) = -i\omega\left(\frac{a}{r}\right)^3[\boldsymbol{\Phi}(\omega)\times\boldsymbol{r}]\frac{1-ikr}{1-ika}e^{ik(r-a)} \tag{1}$$

which determines the external torque $T(\omega) = \alpha^{-1}(\omega)\Phi(\omega)$ to drive the oscillating particle. For small frequencies, the compliance obeys the familiar Stokes result, $\alpha^{-1}/-i\omega = 8\pi a^3\eta$. Deviations from this law occur around $\omega_0 = 2\eta/(\rho a^2)$, *i.e.*, when the penetration depth $\delta = \mathrm{Im}(k)$ equals the particle radius a.

We now study the equivalent problem for a model-viscoelastic medium, represented by a two-fluid model [11]:

$$\mathbf{0} = \mu\nabla^2\boldsymbol{u} + (\lambda+\mu)\nabla(\nabla\cdot\boldsymbol{u}) + \Gamma\left(\boldsymbol{v} - \frac{\partial\boldsymbol{u}}{\partial t}\right), \tag{2}$$

$$\rho\frac{\partial}{\partial t}\boldsymbol{v} = -\nabla p + \eta\nabla^2\boldsymbol{v} - \Gamma\left(\boldsymbol{v} - \frac{\partial\boldsymbol{u}}{\partial t}\right), \quad \mathrm{div}\,\boldsymbol{v} = 0. \tag{3}$$

Here an incompressible Newtonian fluid with shear viscosity η is coupled to an elastic medium with Lamé constants λ, μ via a conventional friction term. By dimensional analysis, the friction coefficient $\Gamma = \eta/\xi^2$ contains a characteristic length ξ which is on the order of the mesh size in, *e.g.*, an actin network [12]. We neglect the mass density of the elastic medium to the one of the Newtonian fluid right from the beginning. The characteristic parameters of the theory are the reduced mesh size ξ/a, $\omega_e = \mu/\eta$ and $\omega_0 = 2\eta/(\rho a^2)$. The two frequencies quantify the fluid inertia, shear elasticity, and shear viscosity. Typical numbers for an actin solution [5] are $\omega_e = 10^3\,\mathrm{Hz}$ and $\omega_0 = 10^5\,\mathrm{Hz}$ based on $a = 3\,\mu\mathrm{m}$, $\eta = 0.01P$ and $\mu = 1\,\mathrm{N/m^2}$.

An oscillating rotating particle creates pure shear fields for both displacement $\boldsymbol{u}$ and velocity $\boldsymbol{v}$ ($\mathrm{div}\,\boldsymbol{u} = \mathrm{div}\,\boldsymbol{v} = 0$) and keeps the pressure constant. One then derives from

eqs. (2) and (3) that the amplitudes $\boldsymbol{u}(\boldsymbol{r},\omega)$ and $\boldsymbol{v}(\boldsymbol{r},\omega)$ of the oscillating fields obey a vector Helmholtz equation in analogy to the pure Newtonian fluid, however with k^2 replaced by a matrix $\boldsymbol{K}^2$. To solve this equation, we introduce

$$\boldsymbol{u}(\boldsymbol{r},\omega) = -a^2\boldsymbol{\Phi}(\omega)\times\nabla g(r) \qquad \text{and} \qquad \boldsymbol{v}(\boldsymbol{r},\omega) = -\omega_e a^2\boldsymbol{\Phi}(\omega)\times\nabla h(r) \tag{4}$$

and finally arrive at the equivalent Helmholtz equation for $g(r)$ and $h(r)$:

$$\left(\overline{\nabla}^2\mathbf{1}+\boldsymbol{K}^2\right)\begin{pmatrix} g(\bar r)\\ h(\bar r)\end{pmatrix} = \mathbf{0} \quad \text{with} \quad \boldsymbol{K}^2 = \frac{a^2}{\xi^2}\begin{pmatrix} i\omega/\omega_e & 1\\ -i\omega/\omega_e & 2i\omega\xi^2/(\omega_0 a^2)-1\end{pmatrix}. \tag{5}$$

The reduced radial coordinate is denoted by $\bar r = r/a$ and the radial part of the Laplace operator reads $\overline{\nabla}^2 = \frac{1}{\bar r^2}\frac{\partial}{\partial \bar r}(\bar r^2\frac{\partial}{\partial \bar r})$. The general solution of eq. (5) is given by $\exp[i\boldsymbol{K}\bar r]/\bar r$ or

$$\begin{pmatrix} g(\bar r)\\ h(\bar r)\end{pmatrix} = \frac{1}{\bar r}\boldsymbol{S}\begin{pmatrix} \exp[i\sqrt{\lambda_1}\bar r] & 0\\ 0 & \exp[i\sqrt{\lambda_2}\bar r]\end{pmatrix}\begin{pmatrix} b_1\\ b_2\end{pmatrix}, \tag{6}$$

where λ_i are the eigenvalues of $\boldsymbol{K}^2$. The matrix $\boldsymbol{S} = (\boldsymbol{e}_1, \boldsymbol{e}_2)$ is composed of the eigenvectors $\boldsymbol{e}_1$ and $\boldsymbol{e}_2$ and therefore diagonalizes $\boldsymbol{K}^2$. Finally, the constants b_i are determined by the boundary conditions on the surface of the particle. Note that the roots $\sqrt{\lambda_i}$ have to be chosen such that the exponentials in eq. (6) decay to zero for large $\bar r$.

In general, the external torque on a particle is calculated by $\boldsymbol{T} = -\int \boldsymbol{r}\times\boldsymbol{\sigma}\,\mathrm{d}\boldsymbol{f}$, where $\boldsymbol{\sigma}$ is the stress tensor and $\mathrm{d}\boldsymbol{f}$ the directed surface element. In our case, $\mathrm{d}\boldsymbol{f} \propto -\boldsymbol{r}$ and the velocity $\boldsymbol{v}$ and displacement vector $\boldsymbol{u}$ point along the azimuthal direction relative to the axis $\boldsymbol{\Phi}(\omega)$. Therefore, only the respective components of the elastic and viscous stress tensor,

$$\sigma^u_{\varphi r} = \mu\left(\frac{\partial u_\varphi}{\partial r} - \frac{u_\varphi}{r}\right) \qquad \text{and} \qquad \sigma^v_{\varphi r} = \eta\left(\frac{\partial v_\varphi}{\partial r} - \frac{v_\varphi}{r}\right), \tag{7}$$

contribute and give a torque parallel to $\boldsymbol{\Phi}(\omega)$ with magnitude $T = T^u + T^v$, where

$$T^u = 8\pi\mu a^3\Phi(\omega)\left(1+\frac{i\omega}{3\omega_e}\left[S_{11}b_1\lambda_1 e^{i\sqrt{\lambda_1}} + S_{12}b_2\lambda_2 e^{i\sqrt{\lambda_2}}\right]\right), \tag{8}$$

$$T^v = -i\omega 8\pi\eta a^3\Phi(\omega)\left(1-\frac{1}{3}\left[S_{21}b_1\lambda_1 e^{i\sqrt{\lambda_1}} + S_{22}b_2\lambda_2 e^{i\sqrt{\lambda_2}}\right]\right). \tag{9}$$

The prefactors on the right-hand side of eqs. (8) and (9) are the Stokes results for a pure elastic or viscous medium.

In the following we consider two cases to determine the constants b_i from the boundary conditions. In the first case, we assume stick boundary conditions for both the viscous and the elastic component at the particle surface, *i.e.*, $\boldsymbol{v} = -i\omega\boldsymbol{u} = -i\omega\boldsymbol{\Phi}(\omega)\times\boldsymbol{r}|_{r=a}$. So we assume that the elastic network is attached to the particle. In the second case, the elastic network is not attached and the elastic stress tensor $\sigma^u_{\varphi r}$ in eqs. (7) vanishes on the particle surface. As a result, the elastic torque T^u is zero and the displacement field has to fulfill the mixed boundary condition $(\partial u_\varphi/\partial r - u_\varphi/r)|_{r=a} = 0$. In both cases, we can write down the solutions in analytic form. However, the concrete formulas are too large to convey direct information. We therefore discuss their graphic representations and determine certain limits.

Case 1. – In figs. 1 and 2 we plot the real and the imaginary part of the inverse compliance $\alpha^{-1}(\omega)$, relative to their results for a pure elastic and viscous system, as a function of ω/ω_e and ω_0/ω_e; the mesh size is $\xi/a = 0.1$. For low frequencies, they both exhibit constant values

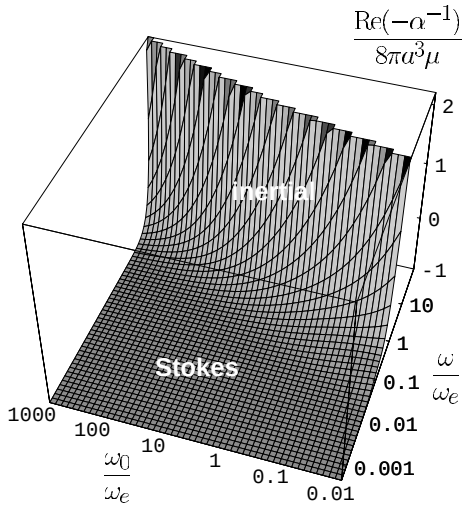

Fig. 1

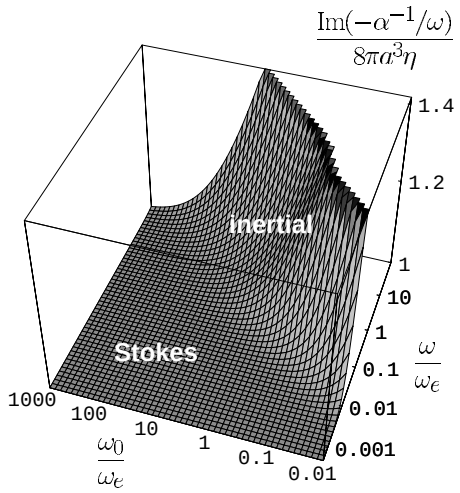

Fig. 2

Fig. 1 – Case 1: real part of the inverse compliance α^{-1}, normalized to $8\pi a^3\mu$ as a function of ω/ω_e and ω_0/ω_e; the parameter is $\xi/a = 0.1$.

Fig. 2 – Case 1: imaginary part of the inverse compliance α^{-1}, normalized to $\omega 8\pi a^3\eta$ as a function of ω/ω_e and ω_0/ω_e; the parameter is $\xi/a = 0.1$.

which correspond to the generalized Stokes relation $\alpha^{-1} = 8\pi a^3 G(\omega)$ with $G(\omega) = \mu - i\omega\eta$. This result can be extracted from our theory as long as the term $2\omega\xi^2/(\omega_0 a^2)$ in the matrix $\boldsymbol{K}^2$ of eq. (5) can be neglected against one, *i.e.*, as long as inertial effects of the fluid are negligible. Note that, unlike the translational motion, the validity of the Stokes relation extends to $\omega \to 0$; there is no lower crossover frequency. The reason is clearly that a rotating sphere only creates pure shear fields for both dynamic variables $\boldsymbol{u}$ and $\boldsymbol{v}$. This indicates that elastic network and viscous fluid are strongly coupled to each other and move together. Therefore, their dynamics is described by the equation of linear elasticity with the complex shear modulus $G(\omega)$ (reminiscent to a Voigt element [3]) or, alternatively, by the Navier-Stokes equation with η replaced by $\eta - \mu/(i\omega)$. With the latter view, the compliance can be calculated using the result from the Newtonian fluid [13] with a complex wave number given by $k^2 = \rho\omega^2/(\mu - i\omega\eta)$:

$$\alpha^{-1}(\omega) = 8\pi a^3 G(\omega)\frac{1 + 2\sqrt{x} + 2x + 2x^{3/2}/3 - i2x(1+\sqrt{x})/3}{1 + 2\sqrt{x} + 2x}, \quad x = \frac{\omega}{\omega_0}\frac{1}{1 + i\omega_e/\omega}. \quad (10)$$

The last equation fits the graphs in figs. 1 and 2 well. It especially accounts for the deviations from the Stokes law due to inertial effects at higher frequencies. In a pure Newtonian fluid, inertia becomes noticeable around the frequency ω_0; just set $\omega_e = \mu/\eta = 0$ in eq. (10). For the strongly coupled viscoelastic system, the onset of inertial effects is not so clear from eq. (10). We therefore determined the appropriate crossover frequencies empirically by requiring that the compliance $\alpha(\omega)$ deviates from the Stokes law by 10%. As is already obvious from the graphs in figs. 1 and 2, we find that the crossover frequencies exhibit different behavior for the real and the imaginary part of $\alpha^{-1}(\omega)$. For the real part, it scales as $\sqrt{\omega_0\omega_e} \propto \mu/(\rho a^2)$, whereas for the imaginary part it behaves as $\omega_0^{0.77}\omega_e^{0.23}$ for $\omega_0/\omega_e < 1$ and passes over to ω_0 for $\omega_0/\omega_e > 1$. This crossover is clearly seen in fig. 2.

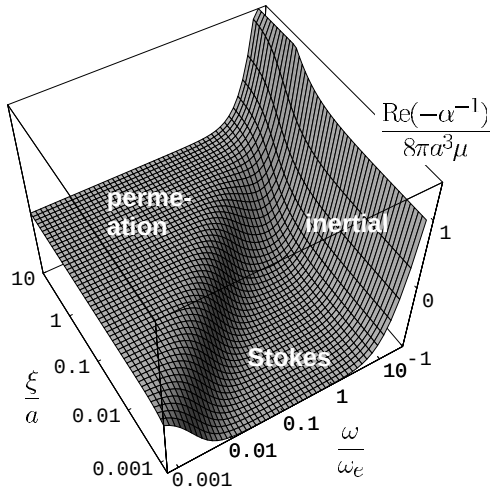

Fig. 3

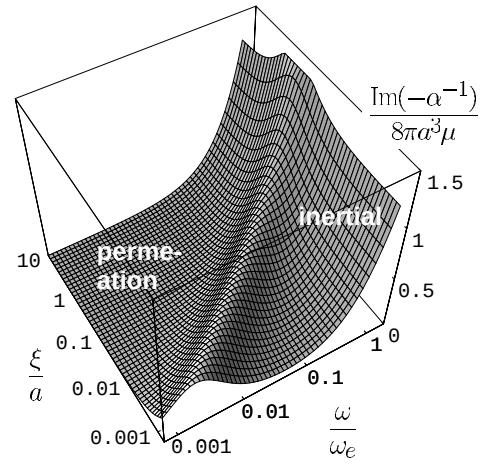

Fig. 4

Fig. 3 – Case 2: real part of the inverse compliance α^{-1}, normalized to $8\pi a^3\mu$ as a function of ω/ω_e and ξ/a; the parameter is $\omega_0/\omega_e = 100$.

Fig. 4 – Case 2: imaginary part of the inverse compliance α^{-1}, normalized to $8\pi a^3\mu$ as a function of ω/ω_e and ξ/a; the parameter is $\omega_0/\omega_e = 100$.

So far, we discussed the case of $\xi/a \ll 1$. For $\xi/a \sim 1$, the regime of generalized Stokes law still exists but eq. (10) does not apply anymore, although the deviations are not dramatic. The regime $\xi/a \sim 1$ means that the continuum limit can no longer be applied to elastic networks such as actin. However, in the two-fluid model ξ just quantifies the frictional coupling between fluid and elastic component. One could wonder if there exists a viscoelastic system with such a weak coupling so that $\xi/a \sim 1$ is applicable.

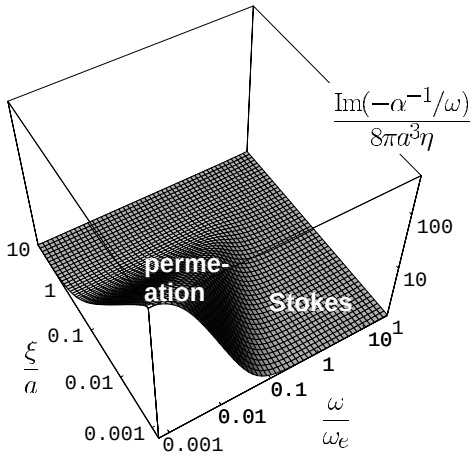

Fig. 5 – Case 2: imaginary part of the inverse compliance α^{-1}, normalized to $\omega 8\pi a^3\eta$ as a function of ω/ω_e and ξ/a; the parameter is $\omega_0/\omega_e = 100$.

Case 2. – We now address the case where the elastic network is not coupled to the particle surface, it only reacts to shear flow via the friction term in eq. (2). In fig. 3, we plot the real part of the inverse compliance as a function of reduced frequency ω/ω_e and mesh size ξ/a; the additional parameter is set to $\omega_0/\omega_e = 100$. For small frequencies, the real part is close to zero, in contrast to case 1, where it assumes the reference Stokes value of $8\pi a^3\mu$, as already discussed. The friction between the two components is sufficiently small so the fluid permeates the elastic network without deforming it noticeably. Then for increasing frequency, an edge occurs and $\mathrm{Re}(\alpha^{-1})$ enters the region where the Stokes law is valid. Note, however, that this region is considerably reduced compared to case 1. Correspondingly, the imaginary part in fig. 4 (also in units of $8\pi a^3\mu$!) exhibits a ridge. This is what we roughly expect since real and imaginary part of the compliance are connected via Kramers-Kronig relations [14]. The features described so far can be explained by the formula

$$\alpha^{-1}(\omega) = 8\pi\mu a^3 \left[\frac{\omega^2\tau^2}{1-i\omega\tau} - i\omega\tau\left(1-\frac{1}{\omega_e\tau}\right)\right] \quad \text{with} \quad \tau = \frac{1}{\omega_e}\frac{a}{3\xi}\sqrt{1-i\omega/\omega_e}\,, \tag{11}$$

which follows from our theory when we neglect again the "inertial term" $2\omega\xi^2/(\omega_0 a^2)$ in the matrix $\boldsymbol{K}^2$ of eq. (5) and set $\xi/a \ll 1$. To determine τ, the complex root with positive real part has to be taken. For $\omega/\omega_e \ll 1$, the existence of the edge and ridge in relation (11) is obvious. Furthermore, the relation demonstrates that edge and ridge, or the onset of the Stokes regime, occur at a frequency which scales as ξ/a. This is in contrast to translational motion where it scales as $(\xi/a)^2$ [5, 12]. In fig. 5 the imaginary part of α^{-1} with proper scale factor $\omega 8\pi a^3\eta$ is plotted. It reveals the strong effect of friction between both components when the fluid permeates the elastic network. Note the logarithmic scale of the vertical axis. Inertial effects for $\xi/a \ll 1$ are again described by eq. (10). So the Stokes regime in fig. 5 extends up to $\omega/\omega_e = 10$ in agreement with fig. 2. Nevertheless, we find that in case 2 the validity of the Stokes law is reduced.

Conclusions. – Based on a two-fluid model, we determined and discussed the compliance for a rotating spherical particle embedded in a viscoelastic medium. In the case where both the viscous and the elastic component obey stick boundary conditions at the particle surface, we identify the validity of a generalized Stokes law, and therefore a simple relation to the complex shear modulus, starting from zero frequency and limited only at high frequencies by inertial effects. This is in contrast to translational motion. When the elastic network is not coupled to the particle, the compliance exhibits a region of low elasticity and high effective viscosity starting from zero frequency, indicating the strong friction which occurs when the fluid permeates the elastic network. The regime of the Stokes law is reduced.

Real viscoelastic systems such as actin solutions possess a frequency-depended complex shear modulus [2, 4, 5]. So to discuss the frequency dependence of the compliance, *e.g.*, in case 1, one has to consider a non-trivial path in figs. 1 and 2 determined by the varying parameter $\omega_0/\omega_e \propto \eta^2(\omega)/\mu(\omega)$. This is, however, no problem in the Stokes regime but leads to additional effects outside the Stokes regime as, *e.g.*, in case 2.

Our study of different boundary conditions clarifies that the interpretation of compliances measured in experiment needs care. So far, in the translational case, stick-boundary conditions are always assumed. Our results show that some slip of the elastic network changes the measurable compliance dramatically. This could lead to false interpretations.

Clearly, one-bead microrheology with rotating particles also suffers from the drawback that it does not probe bulk properties, as is done with the more recently developed two-bead method which measures the correlated motion of two particles [15]. On the other hand, since in the Stokes regime the shear fields decay as $1/r^2$ instead of $1/r$ for translational motion,

rotating particles could be used to monitor explicitly the effect of the embedded beads on the elastic network [16]. A challenge will be to develop the theory for two-bead microrheology including the rotational degree of freedom [17].

In this article we laid the theoretical basis for microrheology with rotating particles. Our results demonstrate that it can be a useful extension of existing methods based on translational motion and also complements them. So we hope that our work stimulates further experimental investigations which use rotating particles as colloidal probes to explore the mechanical properties of soft materials, especially in connection with biological systems.

* * *

The authors thank F. MacKintosh and T. Liverpool for helpful and encouraging discussions. They also acknowledge financial support of the Deutsche Forschungsgemeinschaft under Grant No. Sta 352/5-2 and within the International Graduate College "Soft Matter" and the transregio SFB 6 "Physics of Colloidal Dispersions in External Fields".

REFERENCES

[1] For a review see Gisler T. and Weitz D. A., *Curr. Opin. Colloid Interface Sci.*, **3** (1998) 586; MacKintosh F. C. and Schmidt C. F., *Curr. Opin. Colloid Interface Sci.*, **4** (1999) 300.
[2] Frey E., Kroy K. and Wilhelm J., in *Wiley Polymer Networks Group Review Series*, Vol. **2**, edited by Stokke B. T. and Elgsaeter A. (Wiley, New York) 1999, pp. 287-301.
[3] Ferry J. D., *Viscoelastic Properties of Polymers* (Wiley, New York) 1980.
[4] Palmer A., Mason T. G., Xu J., Kuo S. C. and Wirtz D., *Biophys. J.*, **76** (1999) 1063; Mason T. G., Gisler T., Kroy K., Frey E. and Weitz D. A., *J. Rheol.*, **44** (2000) 917.
[5] Gittes F., Schnurr B., Olmsted P. D., MacKintosh F. C. and Schmidt C. F., *Phys. Rev. Lett.*, **79** (1997) 3286; Schnurr B., Gittes F., MacKintosh F. C. and Schmidt C. F., *Macromolecules*, **30** (1997) 7781.
[6] Bausch A. R., Möller W. and Sackmann E., *Biophys. J.*, **76** (1999) 573.
[7] Ziemann F., Rädler J. and Sackmann E., *Biophys. J.*, **66** (1994) 2210; Amblard F., Maggs A. C., Yurke B., Pargellis A. N. and Leibler S., *Phys. Rev. Lett.*, **77** (1996) 4470.
[8] Mason T. G. and Weitz D. A., *Phys. Rev. Lett.*, **74** (1995) 1250; Mason T. G., Ganesan K., van Zanten J. H., Wirtz D. and Kuo S. C., *Phys. Rev. Lett.*, **79** (1997) 3282; Gisler T. and Weitz D. A., *Phys. Rev. Lett.*, **82** (1999) 1606.
[9] Bishop A. I., Nieminen T. A., Heckenberg N. R. and Rubinsztein-Dunlop H., *Phys. Rev. Lett.*, **92** (2004) 198104; Sandomirski K., Martin S., Maret G., Stark H. and Gisler T., *J. Phys. Condens. Matter*, **16** (2004) S4137.
[10] Cheng Z. and Mason T. G., *Phys. Rev. Lett.*, **90** (2003) 018304.
[11] Brochard F. and de Gennes P. G., *Macromolecules*, **10** (1977) 1157; Milner S. T., *Phys. Rev. E*, **48** (1993) 3674; Stark H. and Trebin H.-R., *Phys. Rev. E*, **51** (1995) 2326.
[12] Levine A. J. and Lubensky T. C., *Phys. Rev. Lett.*, **85** (2000) 1774; *Phys. Rev. E*, **63** (2001) 041510.
[13] Landau L. D. and Lifschitz E. M., *Lehrbuch der Theoretischen Physik, Band VI: Hydrodynamik* (Akademie Verlag, Berlin) 1991.
[14] Chaikin P. M. and Lubensky T. C., *Principles of Condensed Matter Physics* (Cambridge University Press, Cambridge) 1995.
[15] Crocker J. C., Valentine M. T., Weeks E. R., Gisler T., Kaplan P. D., Yodh A. G. and Weitz D. A., *Phys. Rev. Lett.*, **85** (2000) 888; Levine A. J. and Lubensky T. C., *Phys. Rev. E*, **65** (2001) 011501.
[16] MacKintosh F., private communication (2004).
[17] Reichert M. and Stark H., *Phys. Rev. E*, **69** (2004) 031407.